ISSN 1066-3622, Radiochemistry, 2014, Vol. 56, No. 6, pp. 614–621. © Pleiades Publishing, Inc., 2014.
Published in Russian in Radiokhimiya, 2014, Vol. 56, No. 6, pp. 524–530.

Synthesis and Characterization of Polyaniline–Titanium Tungstophosphate; Its Analytical Applications for Sorption of Cs^+, Co^{2+}, and Eu^{3+} from Waste Solutions[1]

Y. F. El-Aryan, H. El-Said, and E. A. Abdel-Galil*

Hot Laboratories Center, Atomic Energy Authority, P.O. Box 13759, Cairo, Egypt
** e-mail: ezzat_20010@yahoo.com*

Received March 4, 2014

Abstract—Crystalline phases of polyaniline–titanium tungstophosphate composite material were synthesized via sol–gel procedure by incorporating the organic polymer polyaniline into the matrix of an inorganic precipitate of titanium tungstophosphate. The physicochemical properties of this hybrid material were determined using atomic absorption spectrophotometry, CHN elemental analysis, X-ray diffraction and X-ray fluorescence analysis, IR spectroscopy, thermal analysis, and scanning electron microscopy. According to the data obtained, the chemical formula of polyaniline–titanium tungstophosphate can be presented as $[(WO_3)(TiO_2)_4(H_3PO_4)_3 + (–C_6H_4NH–)]\cdot 8H_2O$. The material shows monofunctional ion-exchange characteristic and exhibits enhanced resistance to HNO_3, HCl, and alkaline media. The ion-exchange capacity of polyaniline–titanium tungstophosphate for Cs^+, Co^{2+}, and Eu^{3+} ions was found to be 3.63, 1.55, and 1.30 mg-equiv g^{-1}, respectively, exceeding the ion-exchange capacity of other composite and inorganic ion exchangers. The material was found to be highly selective to Eu^{3+}, with the following selectivity series: $Eu^{3+} > Cs^+ > Co^{2+}$. The thermodynamic functions (ΔG^0, ΔS^0, and ΔH^0) of the adsorption of Cs^+, Co^{2+}, and Eu^{3+} ions onto polyaniline–titanium tungstophosphate were calculated. They show that the overall adsorption process is spontaneous and endothermic.

Keywords: synthesis, polyaniline–titanium tungstophosphate, distribution studies, radionuclides, thermodynamic functions

DOI: 10.1134/S106636221406006X

The operation of nuclear power plants, reprocessing plants, and research facilities and the use of radioisotopes in industry and diagnostic medicine produce a wide variety of radioactive wastes [1–3]. These radioactive wastes are generally composed of major quantities of nonradioactive components contaminated with minor amounts of hazardous γ-emitting radionuclides such as ^{137}Cs, ^{60}Co, ^{154}Eu, etc. Many of these wastes have to be treated in order to reduce the radionuclide levels to those acceptable for discharge into the environment. Precipitation, filtration, evaporation, and ion exchange using organic resins are conventional processes used for the treatment. However, organic resins have certain drawbacks, and among them is their ability to swell. Such behavior makes them incompatible with the final waste forms.

Some naturally occurring and/or synthetically prepared inorganic materials have been known for a long time as adsorbents for various radionuclides, mainly alkali and alkaline earth cations [4–6]. The use of inorganic sorbents for treatment of aqueous radioactive wastes may be advantageous because of their thermal and mechanical stability, high radiation resistance, and compatibility with final waste forms [2, 7, 8]. A considerable number of synthetic inorganic sorbents showing strong affinity for one or more radionuclides over a wide pH range have been found. These sorbents are versatile and can be used both in the granular form in a conventional packed-bed installation or in the finely divided form in conjunction with an efficient solid–liquid separation process such as cross-flow filtration [1, 9, 10].

Organic ion exchangers are well known for their uniformity, chemical stability, and control of their ion exchange properties, as well as their characteristic ca-

[1] The text was submitted by the authors in English.

pacities. In order to combine the advantages of polymeric and inorganic materials as ion exchangers, attempts have been made to develop polymeric-inorganic composite ion exchangers by incorporation of organic monomers into an inorganic matrix [11].

In this study, we prepared polyaniline–titanium tungstophosphate composite ion exchanger. The material was characterized by different analytical techniques such as evaluation of thermal and chemical stability, X-ray diffraction (XRD) analysis, and IR spectroscopy. Also, to understand the theoretical aspects of ion-exchange separations and evaluate the practical prospects for using the material for separation of the cations, the thermodynamics functions (ΔG^0, ΔS^0, and ΔH^0) of the adsorption of Cs^+, Co^{2+}, and Eu^{3+} onto polyaniline–titanium tungstophosphate were calculated, and the ion exchange capacity and equilibrium distribution coefficients of metal ions on the material were determined.

EXPERIMENTAL

Chemicals and instruments. The main chemicals used for the synthesis of the material were obtained from BDH (England) and Loba Chemie (India). All the other chemicals were of analytical reagent grade purity and were used without additional purification. pH measurements were performed using a pH meter of model 601A (USA). The CHN elemental analysis was performed with a Flash EA Analyzer (Italy). The inductively coupled plasma atomic absorption spectrophotometer (model ICPS-7500), X-ray diffractometer, and thermal analyzer were from Shimadzu (Kyoto, Japan), and the X-ray fluorescence spectrometer was from Philips (Netherlands).

Preparation of polyaniline–titanium tungstophosphate. 1 M H_3PO_4 and 0.1 M $Na_2WO_4 \cdot 2H_2O$ solutions were prepared in demineralized water (DMW), whereas 0.1 M $TiCl_4$ solution was prepared in 4 M HCl; 10 vol % aniline and 0.1 M $K_2S_2O_8$ solutions were prepared in 1 M HCl. All the solutions were taken for the synthesis in equal volumes.

Polyaniline gels were prepared by mixing 10% aniline and 0.1 M $K_2S_2O_8$ solutions with continuous stirring by a magnetic stirrer. Green polyaniline gels were obtained by keeping the solutions below 10°C for 30 min. Inorganic precipitate of titanium tungstophosphate (TiWP) was prepared by mixing 0.1 M $TiCl_4$, 0.1 M $Na_2WO_4 \cdot 2H_2O$, and 1 M H_3PO_4 solutions at 25°C. The white precipitate formed when the pH of the mixture was adjusted to 0.95 by adding aqueous ammonia. The polyaniline gels were added to the white inorganic precipitate of titanium tungstophosphate with continuous stirring, and the components were thoroughly mixed. The resulting green gel was kept for 24 h at room temperature (25 ± 1°C) for digestion. The supernatant was decanted, and the gel was rewashed with double-distilled water to remove fine adherent particles and was filtered using a centrifuge (about 10^4 rpm) and dried at 50 ± 1°C. The dried products were immersed in DMW to obtain small granules and converted to the H^+ form by treatment with 1 M HNO_3 for 24 h with intermittent shaking and replacement of the supernatant with the fresh acid. The excess acid was removed by several washing with DMW. The product was dried at 50°C and sieved to obtain particles of particular size range (0.12–0.75 mm).

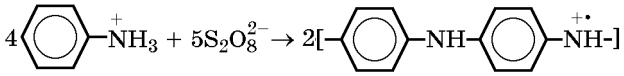

$$+ 12H^+ + 10S_2O_8^{2-},$$

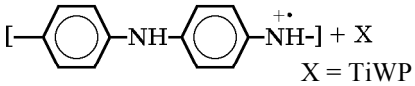

X = TiWP

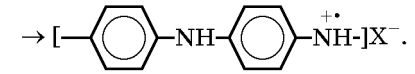

Characterization of the prepared polyaniline–titanium tungstophosphate. Some physical and chemical properties of the prepared polyaniline–titanium tungstophosphate (PA–TiWP) were examined by X-ray diffraction (XRD), X-ray fluorescence spectrometry (XRF), IR spectroscopy, scanning electron microscopy (SEM), and thermal analysis (TGA and DTA).

pH titration. The pH titration of PA–TiWP was carried out as follows: 0.3 g of the material was placed in a column fitted with glass wool at its bottom. A glass bottle containing 50 mL of 0.001 M HCl was placed below the column, and for pH determination, a glass electrode was placed in the solution. Then, 100 mL of 0.01 M LiOH, NaOH, or KOH was poured into the column. Titration was carried out by passing the alkali metal hydroxide solution at a rate of about 10 drops per minute until pH ~10 was reached [8].

Chemical stability. The chemical stability of PA–TiWP was studied in water, acid (HNO_3, HCl) solu-

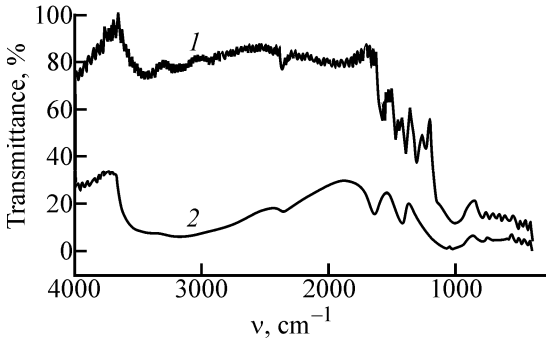

Fig. 1. IR spectra of (*1*) PA–TiWP and (*2*) TiWP after drying at 50°C.

tions of different concentrations (0.5, 1, 2, 3, and 4 M), and base (KOH, NaOH) solutions of different concentrations (0.1 and 1 M). A 100-mg portion of a PA–TiWP sample was kept in contact with 100 mL of the desired solution with intermittent shaking for approximately 1 week at 25 ± 1°C.

Capacity measurements. The PA–TiWP capacity was determined by the batch technique. A 0.1-g portion of the solid material was equilibrated with 10 mL of a solution of Cs^+, Co^{2+}, and/or Eu^{3+} chlorides (ionic strength about 0.1) at the V/m ratio of 100 mL g^{-1}. The mixture was shaken in a shaker thermostat at 25 ± 1°C and left overnight. After that, the solid was separated, and the concentration of the metal ions was measured by ICP-AAS. The capacity A (mg-equiv g^{-1}) was calculated by the formula

$$A = \sigma C_0(V/m)Z, \quad (1)$$

where σ is the degree of the ion uptake, C_0 the initial concentration of the ions in the solution (M), V is the solution volume (mL), m is the sorbent weight (g), and Z is the valence of the exchanged ions.

Table 1. Band frequencies (cm^{-1}) in the IR spectra of PA–TiWP and TiWP and their assignment

PA–TiWP	TiWP	Calculation [18, 19]	Assignment
3419	3419		ν(OH) and ν(H_2O)
3174		3171	$\nu_s(NH_2)$
2917			ν(C–H)
1566	1629		δ(H_2O)
1552			δ(N–H)
1478	1405		δ(M–OH)
1303			ν(C–N)
1241		1208	ω(NH_2)
792–1015	799–1015		PO_4^{3-}, HPO_4^{2-}, $H_2PO_4^-$
510, 585	510, 603		M–O

Distribution studies. The distribution coefficients (K_d) of Cs^+, Co^{2+}, and Eu^{3+} ions on PA–TiWP were determined by batch equilibration in relation to the HCl concentration. A 0.1-g portion of the prepared ion exchanger was shaken with 10 mL of a 10^{-3} M solution of the above-mentioned metal ions (V/m = 100 mL g^{-1}). The mixture was left overnight (time in which the equilibrium was attained) in a shaker thermostat adjusted at 25 ± 1°C. After equilibration, the solutions were separated by centrifugation, the residual concentration of metal ions in the solution was determined, and the amount of the sorbed ions was determined from the difference between the initial and residual concentrations of the metal ions in the solution. The pH values were also measured before and after equilibration. All the tests were repeated two or three times, and the overall experimental uncertainty was about ±3%.

The distribution coefficients (K_d) were calculated by the formula

$$K_d = [(C_0 - C_{eq})/C_{eq}](V/m), \quad (2)$$

where C_0 and C_{eq} are the concentrations of the ions in solution before and after equilibration, respectively.

The separation factor characterizes the relative tendency of two ions to be adsorbed onto an exchanger from solutions of equal concentration. It is used as a measure of the possibility of chromatographic separation and is calculated as the ratio of the distribution coefficients of elements A and B being separated:

$$\alpha^{A/B} = K_d^A/K_d^B. \quad (3)$$

Water content. The water content of PA–TiWP in the H^+, Cs^+, Co^{2+}, and Eu^{3+} forms was determined by thermal analysis (TGA and DTA) and was found to be 31.08, 34.33, 35.73, and 38.65%, respectively.

Chemical composition. The material was analyzed for Ti(IV), W, and phosphate by X-ray fluorescence spectrometry and for carbon, hydrogen, and nitrogen by elemental analysis. The composition of the material was as follows (wt %): Ti 30.93, W 27.21, PO_4^{3-} 14.91, C 11.64, H 3.20, and N 1.12.

RESULTS AND DISCUSSION

The IR spectrum of titanium tungstophosphate is given in Fig. 1 and Table 1. The peak at 3419 cm^{-1} is

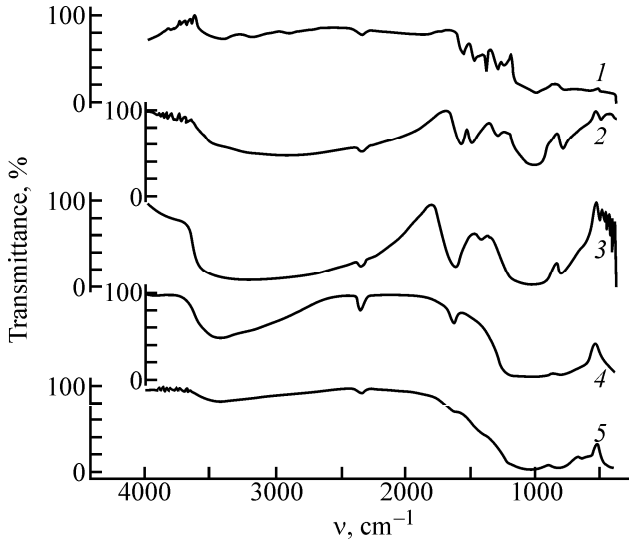

Fig. 2. IR spectra of PA–TiWP after drying at (*1*) 50, (*2*) 200, (*3*) 400, (*4*) 600, and (*5*) 850°C.

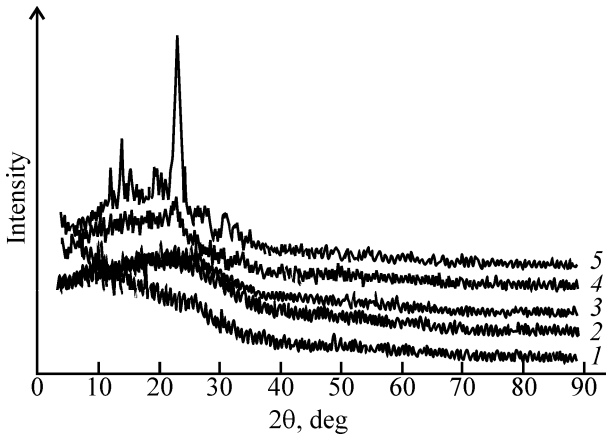

Fig. 3. X-ray diffraction patterns of the PA–TiWP samples after drying at (*1*) 50, (*2*) 200, (*3*) 400, (*4*) 600, and (*5*) 850°C.

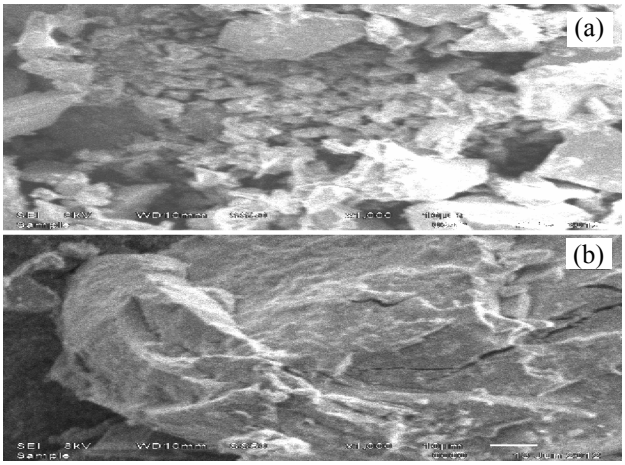

Fig. 4. SEM images of (a) TiWP and (b) PA–TiWP.

characteristics of the stretching mode of free water adsorbed on titanium tungstophosphate and of OH groups [12, 13, 18, 19]. The peak at 1629 cm^{-1} represents the bending mode of water molecules [13]. The peak at 1405 cm^{-1} is due to the bending vibration of hydroxyl groups (Ti–OH) [14, 20]. The peaks at 799 and 1015 cm^{-1} are due to phosphate group (the presence of PO_4^{3-}, HPO_4^{2-}, and $H_2PO_4^{2-}$ is possible) [13, 20, 21]. The peaks at 510 and 603 cm^{-1} can be assigned to metal–oxygen bonds [16, 17].

The IR spectrum of PA–TiWP is also given in Fig. 1 and Table 1. Along with all the above-mentioned absorption bands, it contains five new absorption bands at 1241, 1303, 1552, 2917, and 3174 cm^{-1}, caused by $\omega(NH_2)$ vibrations [18–20], C–N stretching vibrations [15], N–H bending vibrations [15], C–H stretching vibrations, and symmetric stretching vibrations of the NH_2 group [$\nu_s(NH_2)$] [18–20], respectively. The results obtained indicate that the product contains large amount of aniline.

For all the samples, the intensity of the H_2O vibration bands at 3419 and 1566 cm^{-1} decreased as the heating temperature was increased from 50 to 850 ± 1°C (Fig. 2). The polyaniline bands disappeared at 400°C, which is consistent with the results of thermogravimetric analysis (see below).

As seen from Fig. 3, the PA–TiWP sample heated at 50 ± 1°C is X-ray amorphous. On heating from 50 to 400 ± 1°C, the crystal structure is not formed. Signs of the crystal structure formation appear only at 600°C, and at 850 ± 1°C the crystallinity is sharply improved.

The SEM images of TiWP and PA–TiWP are shown in Fig. 4. They illustrate binding of the inorganic ion-exchange titanium tungstophosphate material with the organic polymer, polyaniline. This binding leads to changes in the morphology.

Figure 5 shows the pH titration curves of PA–TiWP with a 0.01 M alkali metal hydroxide (LiOH, NaOH, or KOH) solution. The data are given per gram of the material. The pH titration curve has only one inflection point, indicating that the prepared PA–TiWP behaves as monofunctional ion exchanger. This behavior is similar to that of polyacrylamide–Sn(IV) molybdophosphate prepared by El-Naggar et al. [20], polyaniline–silicotitanate prepared by El-Naggar et al. [22], cerium(IV) molybdate prepared by Nilchi et al [8], ZrP-001 prepared by Pan et al. [23], stannic silico-

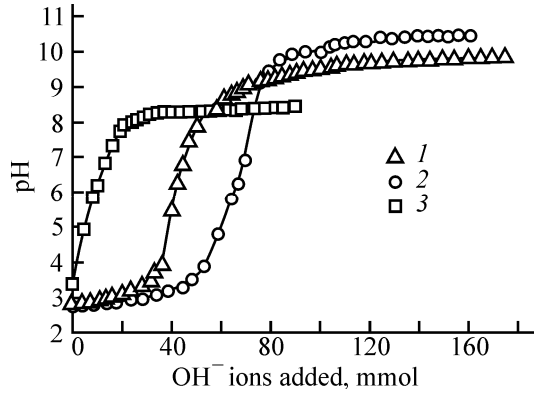

Fig. 5. pH titration curves of PA–TiWP with solutions of alkali metal hydroxides. Alkali metal: (*1*) Li, (*2*) Na, and (*3*) K.

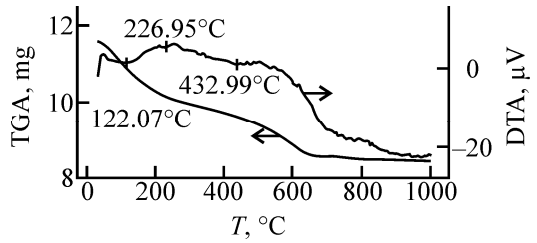

Fig. 6. TGA and DTA curves for the as-prepared sample of PA–TiWP.

molybdate prepared by Nabi and Khan [24], and titanium vanadate prepared by El-Naggar et al. [25]. PA–TiWP behaves as a strongly acidic cation exchanger, as indicated by low pH (~3) of the solution before the start of the titration. The H^+–Na^+ exchange is faster than the H^+–Li^+ and H^+–K^+ exchange. With respect to the tendency to adsorption onto PA–TiWP in acidic and basic media, the alkali metal ions can be ranked in the following order: Na(I) > Li(I) > K(I).

Table 2. Dissolution of PA–TiWP, g L^{-1}, in acids and alkalis at 25 ± 1°C[a]

Concentration, M	HNO_3	HCl	KOH	NaOH
0.1	–	–	0.093	0.091
0.5	0.043	0.050	–	–
1	0.072	0.106	0.100	0.097
2	0.116	0.135	–	–
3	0.120	0.138	–	–
4	0.130	0.142	–	–

[a] The solubility in pure water is below the detection limit.

Table 3. Ion-exchange capacity of PA–TiWP for Cs^+, Co^{2+}, and Eu^{3+} ions

Ion	pH of solution	Ionic radius, Å	Hydration energy, kJ mol^{-1}	Capacity, mg-equiv g^{-1}
Eu^{3+}	4.71	0.95	–	3.630
Cs^+	4.61	1.67	263	1.550
Co^{2+}	4.32	0.72	2054	1.300

Thermogravimetric study of the as-prepared sample of PA–TiWP was also carried out in air with heating to 1000°C at a constant rate of ~10 deg min^{-1}. The results are shown in Fig. 6. On heating to 175°C, the weight loss is 9.79%. It is probably associated with the loss of external water molecules [26]. The corresponding endothermic peak in the DTA curve is observed at 122.07°C. A slow weight loss of about 2.80% observed between 191 and 268°C may be due to the condensation of phosphate group to pyrophosphate groups [27]. The corresponding endothermic peak in the DTA curve is observed at 226.95°C. Further weight loss (~6.81%) on heating to 536°C may be due to complete decomposition of the organic component [20, 28, 29] (endothermic peak at 433°C). From 674°C onwards, there is no weight loss, i.e., the formation of the oxide form of the material is complete [25, 27].

The solubility experiments show that the material has reasonably good chemical stability in solutions of acids (HNO_3, HCl) and alkalis (KOH, NaOH) (Table 2).

Polyaniline–titanium tungstophosphate is more stable than titanium tungstophosphate prepared by Siddiqi and Pathania [30], especially in alkaline media (0.1, 1 M NaOH and KOH), polyacrylamide–Sn(IV) molybdophosphate prepared by El-Naggar et al. [20], polypyrrole–Th(IV) phosphate prepared by Khan et al. [28], polyaniline–Sn(IV) tungstoarsenate prepared by Khan and Alam [29], polypyrrole/polyantimonic acid prepared by Khan and Alam [31], polyaniline–Sn(IV) arsenophosphate prepared by Niwas et al. [32] (in alkaline solutions: 0.1 and 1 M NaOH and KOH), but less stable than polyaniline–Sn(IV) phosphate prepared by Khan and Inamuddin [27] and polyaniline–Sn(IV) arsenophosphate prepared by Niwas et al. [32] (in acid solutions: 1 and 4 M HCl and HNO_3).

The ion-exchange capacity of PA–TiWP depends on the size and charge of the exchanging ion. It increases with a decrease in the radius of the hydrated ion and in the hydration energy [33–35] (Table 3).

PA–TiWP surpasses other composite and inorganic ion exchangers [20, 36–42] in the ion-exchange capacity.

The pH dependence of the ion-exchange capacities of PA–TiWP for Cs^+, Co^{2+}, and Eu^{3+} ions at a constant ionic strength (0.1) was also studied. As seen from Fig. 7, the capacity for these ions increases with pH, which may be due to facilitated release of H^+ ions from the exchanger into the solution.

The capacity–pH curve of PA–TiWP has a single inflection point (Fig. 7). This means that PA–TiWP behaves as a monofunctional material, which is consistent with the results of pH titration (Fig. 5).

Distribution Studies

The $\log K_d$–pH dependences for Cs^+, Co^{2+}, and Eu^{3+} are shown in Fig. 8 and Table 4. The distribution coefficient K_d increases with pH. At low pH values, with an increase in the concentration of H^+ ions the mobility of the Cs^+, Co^{2+}, and Eu^{3+} ions decreases, which can be attributed to an increase in the frictional forces acting on the ions due to the change in the nature of hydrogen bonds in water [43]. As the proton concentration is increased, the following water cluster ions are formed: H_3O^+, $H_5O_2^+$, $H_7O_3^+$, and $H_9O_4^+$, modifying the structure of water and thus the ion–water interaction [43]. Also, the sorbent takes up the H^+ ions from the solution; hence, the surface becomes positively charged, which eventually restricts the uptake of Cu^{2+}, Zn^{2+}, Cd^{2+}, and Pb^{2+} ions [43]. With increasing pH, the adsorption percentage increased substantially. This increase was attributed to hydrolytic adsorption of ions [43]. On the other hand, the linear plots of $\log K_d$ vs. pH, observed for Cs^+, Co^{2+}, and Eu^{3+} ions, have the slopes of 0.337, 0.123, and 0.229, respectively. These slopes do not correspond to the valence of the metal ions sorbed, i.e., the exchange reaction is not ideal. These results cannot be rationalized only in terms of electrostatic interaction between the hydrated cations and the anionic sites in the exchanger. Therefore, it can be assumed that the pH dependence of K_d of cations is determined not only by purely Coulombic interaction with the anionic sites, but also by the formation of covalent bonds as, e.g., in weakly acidic resins containing carboxylic or phosphoric acid groups. Such interaction is closely related to the ionic potential of the cations [20, 44]. The following selectivity order in sorption of cations onto PA–TiWP under indentical conditions was obtained: $Eu^{3+} > Cs^+ > Co^{2+}$.

This sequence is in accordance with the hydrated ionic radii and hydration energy of the exchanged ions. The ions with smaller hydrated ionic radii and hydration energy are exchanged more easily and move faster

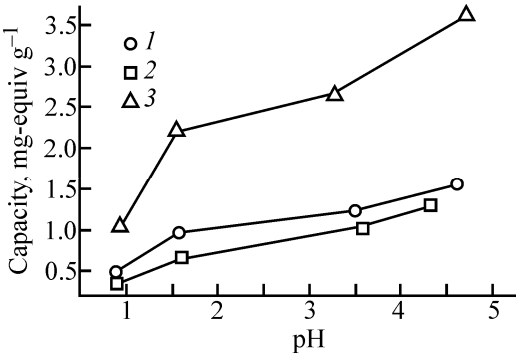

Fig. 7. Plots of capacity vs. pH for the exchange of (*1*) Cs^+, (*2*) Co^{2+}, and (*3*) Eu^{3+} ions on PA–TiWP at 25 ± 1°C.

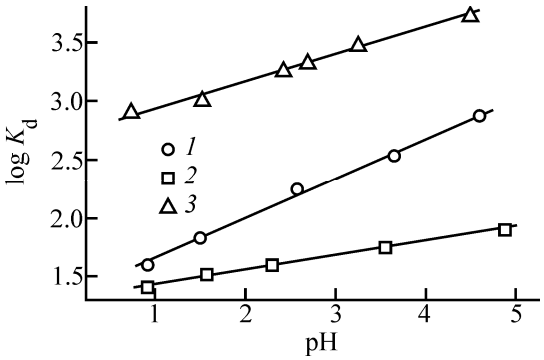

Fig. 8. Plot of $\log K_d$ for (*1*) Cs^+, (*2*) Co^{2+}, and (*3*) Eu^{3+} on PA–TiWP vs. pH at 25°C.

than that the ions with larger ionic radii [20, 25]. The distribution coefficients obtained on PA–TiWP appear to be higher than those obtained on a number of other composite and inorganic ion exchangers [20, 36, 37, 39–41, 45, 46] but lower than, e.g., those of Cs^+ and Co^{2+} ions on titanium vanadate [25] and those of Cs^+ ions on poly(acrylamide–acrylic acid)–montmorillonite [47].

The separation factors α of Cs^+, Co^{2+}, and Eu^{3+} ions on PA–TiWP at different pH values are also given in Table 4. As can be seen, the separation factors of Eu^{3+} from the other metal ions are larger than those of Cs^+ and Co^{2+}. This fact can be used for the separation of

Table 4. Distribution coefficients K_d of Cs^+, Co^{2+} and Eu^{3+} and separation factors $\alpha^{Cs,Co/Eu}$ (in parentheses) and $\alpha^{Co/Cs}$ (in square brackets) on PA–TiWP in relation to pH

pH	Eu^{3+}	Cs^+	Co^{2+}
0.91	832	41.7 (20.0)	25.1 (33.1) [1.66]
1.50	1143	67.6 (16.9)	31.0 (36.8) [2.18]
2.30	1710	123 (13.9)	39.8 (43) [3.1]
3.26	3025	269 (11.2)	51.3 (59) [5.3]
4.48	5456	681 (8.0)	72.1 (76) [9.4]

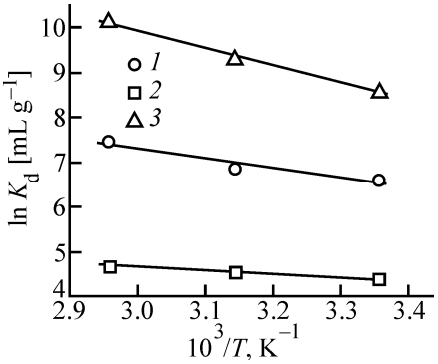

Fig. 9. Van't Hoff plots for the adsorption of (*1*) Cs^+, (*2*) Co^{2+}, and (*3*) Eu^{3+} ions onto PA–TiWP.

the Eu^{3+}–Cs^+ and Eu^{3+}–Co^{2+} pairs at pH 0.91, 1.50, 2.30, 3.26, and 4.48. The Cs^+–Co^{2+} separation is also possible, especially at high pH values. Thus, PA–TiWP can be used for removing these radioactive nuclides from waste streams.

Figure 9 shows the linear relationship between $\ln K_d$ and $1/T$ in accordance with the van't Hoff relationship:

$$\ln K_d = \Delta S^0/R - \Delta H^0/(RT), \quad (4)$$

where ΔS^0 is the entropy change, ΔH^0 is the enthalpy change, R is the gas constant, and T is the absolute temperature.

We found that the distribution coefficients K_d of Cs^+, Co^{2+}, and Eu^{3+} on PA–TiWP increased with an increase in temperature from 298 to 338 K (i.e., decreased with an increase in $1/T$). This trend can be attributed to acceleration of some originally slow adsorption steps and creation of some new active sites on the adsorbent surfaces [20, 48, 49]. From the slopes and intercepts of these straight lines (Fig. 9), we calculated ΔH^0 and ΔS^0 (Table 5), and from the equation

Table 5. Thermodynamic functions of adsorption of Cs^+, Co^{2+}, and Eu^{3+} ions on PA–TiWP

Ion	T, K	ΔG^0, kJ mol^{-1}	ΔH^0, kJ mol^{-1}	ΔS^0, J mol^{-1} K^{-1}
Cs^+	298	–16.369	17.503	113.664
	318	–18.197		112.264
	338	–20.935		113.720
Co^{2+}	298	–10.827	6.684	58.760
	318	–11.950		58.590
	338	–13.179		58.760
Eu^{3+}	298	–21.307	31.950	178.710
	318	–24.614		177.870
	338	–28.466		178.740

$$\Delta G^0 = -RT\ln K_d, \quad (5)$$

the free energy of the adsorption.

The positive values of ΔH^0 indicate that the adsorption is endothermic [25], while the positive values of ΔS^0 for Cs^+, Co^{2+}, and Eu^{3+} suggest increased randomness at the solid–solution interface during the adsorption of these cations on PA–TiWP. The negative values of ΔG^0 indicate that the adsorption is spontaneous and that the cations studied are adsorbed preferentially relative to H^+. The negative value of ΔG^0 decreases in the order $Eu^{3+} > Cs^+ > Co^{2+}$, which agrees with the selectivity order of PA–TiWP for these cations.

According to the analysis results, the molar ratio of Ti(IV), W, PO_4^{3-}, C, H, and N in the material is 4.05 : 1 : 3.01 : 6.05 : 20 : 0.5, which allows the material formula to be tentatively written as follows:

$$[(WO_3)(TiO_2)_4(H_3PO_4)_3 + (-C_6H_4NH-)]\cdot nH_2O.$$

Assuming that only the external water molecules are lost at temperatures of up to 175°C and taking into account that the weight loss at this temperature is 9.79% (TGA data), we can estimate n using Alberti's equation [50]

$$18n = X(M + 18n)/100,$$

where X is the weight loss (%) of the exchanger on heating to 175°C and M is the molecular weight of the anhydrous material. The calculations give $n \approx 8$.

Thus, we have prepared an inorganic hybrid material exhibiting enhanced stability in acid and alkaline solutions and increased ion-exchange capacity, compared to other composite ion exchangers. The selective behavior of this material is important from the environmental pollution chemistry point of view. It allows efficient separation of Eu(III) from other radioactive pollutants.

REFERENCES

1. Kemp, R.V., Bennett, D.G., and White, M.J., *Environ. Int*., 2006, vol. 32, no. 8, pp. 1021–1032.
2. Plećaš, I. and Dimovic, S., *Prog. Nucl. Energy*, 2006, vol. 48, no. 7, pp. 629–633.
3. Borovinskii, V.A., Lyzlova, E.V., and Ramazanov, L.M., *Radiochemistry*, 2001, vol. 43, no. 1, pp. 84–86.
4. Nilchi, A., Khanchi, M., and Ghanadi Maragheh, M., *Talanta*, 2002, vol. 56, p. 383.
5. Shady, S.A. and El-Gammal, B., *Colloids Surf. A: Physicochem. Eng. Aspects*, 2005, vol. 268, pp. 7–11.
6. El-Said, H., Ramadan, H.E., El-Amir, M.A., and Sha-

dy, S.A., *Radiochemistry*, 2012, vol. 54, no. 6, pp. 573–577.
7. Sarma, K.H., Fourcade, J., Lee, S.-G., and Solomon, A.A., *J. Nucl. Mater*., 2006, vol. 352, nos. 1–3, pp. 324–333.
8. Nilchi, A., Maalek, B., Khanchi, A., et al., *Radiat. Phys. Chem*., 2006, vol. 75, no. 2, pp. 301–308.
9. Hooper, W., in Use of inorganic sorbents for treatment of liquid radioactive waste and backfill of underground repositories, *IAEA TECDOC 675*, Vienna: IAEA, 1992, p. 69.
10. Klisuranov, G.S., Gradev, G., Stefanova, I., and Milusheva, A., in Use of inorganic sorbents for treatment of liquid radioactive waste and backfill of underground repositories, *IAEA TECDOC 675*, Vienna: IAEA, 1992, p. 15.
11. El-Naggar, I.M., Ibrahim, G.M., El-Kady, E.A., and Hegazy, E.A., *Desalination*, 2009, vol. 237, pp. 147–154.
12. Roganarasimhan, S.R., *Indian J. Chem*., 1963, vol. 18, p. 360.
13. Rao, C.N.R., *Chemical Applications of Infrared Spectroscopy*, New York: Academic, 1963.
14. Nabi, S.A., Naushad, M., and Inamuddin, *J. Hazard. Mater*., 2007, vol. 142, pp. 404–411.
15. El-Naggar, I.M., Zakaria, E.S., Ali, I.M., et al., *Arab. J. Chem*., 2012, vol. 5, pp. 109–119.
16. Nabi, S.A. and Siddiqui, Z.M., *Bull. Chem. Soc. Jpn*., 1985, vol. 58, pp. 724–730.
17. Rawat, J.P. and Ansari, A.A., *Bull. Chem. Soc. Jpn*., 1990, vol. 63, p. 1521.
18. Mohan, S. and Murugan, R., *Arab. J. Sci. Eng., Sect. A*, 1997, vol. 22, no. 2A, pp. 155–164.
19. Murugan, R., Mohan, S., and Bigotto, A., *J. Korean Phys. Soc*., 1998, vol. 32, no. 4, pp. 505–512.
20. El-Naggar, I.M., Mowafy, E.A., Abdel-Galil, E.A., and El-Shahat, M.F., *Global J. Phys. Chem*., 2010, vol. 1, no. 1, pp. 91–106.
21. Vesely, V. and Pekarek, V., *J. Inorg. Nucl. Chem*., 1963, vol. 25, p. 697.
22. El-Naggar, I.M., Hebash, K.A., Sheneshen, E.S., and Abdel-Galil, E.A., *Inorg. Chem. Indian J.*, 2014, vol. 9, no. 1, pp. 1–14.
23. Pan, B.C., Zhang, Q.R., Zhang, W.M., et al., *J. Colloid Interface Sci*., 2007, vol. 310, pp. 99–105.
24. Nabi, S.A. and Khan, A.M., *React. Funct. Polym*., 2006, vol. 66, pp. 495–508.
25. El-Naggar, I.M., Zakaria, E.S., El-Kenany, W.M., and El-Shahat, M.F., *Radiochemistry*, 2014, vol. 56, no. 1, pp. 86–91.
26. Duval, C., *Inorganic Thermogravimetric Analysis*, Amsterdam: Elsevier, 1963, p. 315.
27. Khan, A.A. and Inamuddin, *React. Funct. Polym*., 2006, vol. 66, pp. 1649–1663.
28. Khan, A.A., Inamuddin, and Alam, M.M., *Mater. Res. Bull*., 2005, vol. 40, pp. 289–305.
29. Khan, A.A. and Alam, M.M., *React. Funct. Polym*., 2003, vol. 55, pp. 277–290.
30. Siddiqui, Z.M. and Pathania, D., *J. Chromatogr. A*, 2003, vol. 987, pp. 147–158.
31. Khan, A.A. and Alam, M.M., *Anal. Chim. Acta*, 2004, vol. 504, pp. 253–264.
32. Niwas, R., Khan, A.A., and Varshney, K.G., *Colloids Surf. A: Physicochem. Eng. Aspects*, 1999, vol. 150, pp. 7–14.
33. Nabi, S.A., Islam, A., and Rahman, N., *Ann. Chim. Sci. Mater*., 1997, vol. 22, pp. 463–473.
34. Rawat, J.P. and Singh, J.P., *Can. J. Chem*., 1976, vol. 54, pp. 2534–2539.
35. Borgo, C.A., Lazarin, A.M., Kholin, Y.V., et al., *J. Braz. Chem. Soc*., 2004, vol. 15, pp. 50–57.
36. Ali, I.M., Zakaria, E.S., Ibrahim, M.M., and El-Naggar, I.M., *Polyhedron*, 2008, vol. 27, pp. 429–439.
37. El-Naggar, I.M. and Abou-Mesalam, M.M., *J. Hazard. Mater*., 2007, vol. 149, pp. 686–692.
38. El-Gammal, B. and Shady, S.A., *Colloids Surf. A: Physicochem. Eng. Aspects*, 2006, vol. 287, pp. 132–138.
39. Lahiri, S., Roy, K., Bhattacharya, S., et al., *Appl. Radiat. Isot*., 2005, vol. 63, pp. 293–297.
40. El-Naggar, I.M., Mowafy, E.A., Abdel-Galil, E.A., and Ghonaim, A.Kh., *Arab J. Nucl. Sci. Appl*., 2008. vol. 41, N 3. P. 1–14.
41. Aly, H.F., Zakaria, E.S., Shady, S.A., and El-Naggar, I.M., *J. Radioanal. Nucl. Chem*., 1999, vol. 241, no. 2, pp. 331–336.
42. El-Naggar, I.M., Zakaria, E.S., Shady, S.A., and Aly, H.F., *Solid State Ionics*, 1999, vol. 122, pp. 65–70.
43. Moloukhia, H., *J. Radiat. Res. Appl. Sci*., 2010, vol. 3, no. 2, pp. 343–356.
44. Ahrland, S., Albertsson, J., Johansson, L., et al., *Acta Chem. Scand*., 1964, vol. 18, p. 707.
45. Mittal, S.K., Sharma, H.K., and Ashok, S.K., *React. Funct. Polym*., 2006, vol. 66, pp. 1174–1181.
46. Yavari, R., Khanchi, A.R., Maragheh, M.G., and Waqif-Husain, S., *J. Radioanal. Nucl. Chem*., 2006, vol. 267, no. 3, pp. 685–690.
47. El-Said, H., El-Amir, M.A., Abdel-Aziz, H.M., and Siyam, T., *Radiochemistry*, 2012, vol. 54, no. 3, pp. 269–273.
48. Clark, A., *Theory of Adsorption and Catalysis*, New York: Academic, 1970.
49. Mishra, S.P., Singh, U.K., and Tiwari, D., *J. Radiat. Chem*., 1996, vol. 210, p. 207.
50. Alberti, G., Torracca, E., and Conte, A., *J. Inorg. Nucl. Chem*., 1966, vol. 28, pp. 607–613.